Lepton PDFs and multipurpose single-lepton searches at the LHC

Herbi K. Dreiner,[1,*] Víctor Martín Lozano,[2,3,†] Saurabh Nangia,[1,‡] and Toby Opferkuch[4,5,6,§]

[1]*Bethe Center for Theoretical Physics and Physikalisches Institut der Universität Bonn, Nußallee 12, 53115 Bonn, Germany*

[2]*Deutsches Elektronen-Synchrotron DESY, Notkestrasse 85, 22607 Hamburg, Germany*

[3]*Departament de Física Teòrica and IFIC, Universitat de València-CSIC, E-46100 Burjassot, Spain*

[4]*Berkeley Center for Theoretical Physics, University of California, Berkeley, California 94720, USA*

[5]*Theoretical Physics Group, Lawrence Berkeley National Laboratory, Berkeley, California 94720, USA*

[6]*Theoretical Physics Department, CERN, Esplanade des Particules, 1211 Geneva 23, Switzerland*

(Received 14 July 2022; accepted 24 January 2023; published 13 February 2023)

A final state consisting of one charged lepton, at least one jet, and little missing transverse energy can be a very promising signature of new physics at the LHC across a wide range of models. However, it has received only limited attention so far. In this work we discuss the potential sensitivity of this channel to various new physics scenarios. To demonstrate our point, we consider its application to lepton parton distribution functions (PDFs) at the LHC in the context of supersymmetry. These lepton PDFs can lead to resonant squark production (similar to leptoquarks) via lepton number violating couplings present in R-parity violating supersymmetry (RPV-SUSY). Unlike leptoquarks, in RPV-SUSY there are many possible decay modes leading to a wide range of signatures. We propose two generic search regions: (a) a single first or second generation charged lepton, exactly 1 jet and low missing transverse energy, and (b) a single first or second generation charged lepton, at least 3 jets, and low missing transverse energy. We demonstrate that together these cover a large range of RPV-SUSY signatures, and have the potential to perform better than existing low-energy bounds, while being general enough to extend to a wide range of possible models hitherto not explored at the LHC.

DOI: 10.1103/PhysRevD.107.035011

I. INTRODUCTION

With the high-luminosity (HL) era almost upon us, the Large Hadron Collider (LHC) is gearing up for a paradigm shift: a transition from energy upgrades to a focus on increased luminosity. The LHC has already accumulated close to 200 fb^{-1} of data [1]. This will be surpassed in just a single year of HL-LHC runtime, which by its conclusion will increase the total integrated luminosity by a factor 15 overall [2].

Given the breadth of possible observables, such a drastic increase in integrated luminosity places a renewed importance in exploring the question, "Where should we look for new physics?" In contrast to an increase in energy, increases in luminosity do not typically yield dramatic improvements in reach when considering resonantly produced new physics. On the other hand, rare processes, indirect searches, and new trigger techniques—to which the experiments are currently insensitive with the data on tape—can offer promising avenues to explore; current examples include Refs. [3–8]. Such strategies can be more powerful than one may expect. In this work we demonstrate this point explicitly by making the case for a specific example of an unusual signal at the LHC: one light charged lepton, one light jet, and no missing energy—what we will call the *single-lepton channel*.

We mention that an interesting aspect of the kind of lepton-number violating searches we discuss is the fact that they could also be relevant to current topics of interest such as the B-anomalies [9,10], and the muon $(g-2)$ [11–14]; the variety of models that produce signals of interest to us may also explain these anomalies (see for example Refs. [15–19]).

The outline of this paper is as follows. In Sec. II, we discuss the single-lepton channel in detail, and argue that it can be applied to a wide range of models with lepton number violating interactions. Section III discusses its application to the specific context of RPV-SUSY. In Sec. IV, we demonstrate how such a search for RPV-SUSY may be implemented at the LHC. In Sec. V, we

*dreiner@uni-bonn.de
†victor.lozano@ific.uv.es
‡nangia@physik.uni-bonn.de
§toby.opferkuch@cern.ch

present and discuss our numerical results. We conclude in Sec. VI.

II. THE SINGLE-LEPTON CHANNEL

The final state we are interested in has exactly one energetic[1] first or second generation charged lepton (ℓ), at least one energetic light jet (j), and little or no missing transverse energy ($E_{\mathrm{T}}^{\mathrm{miss}}$). In what follows we refer to this as the single-lepton channel for short.

At first glance this channel is forbidden at hadron colliders in the limit $E_{\mathrm{T}}^{\mathrm{miss}} \to 0$ as the final state is odd in lepton number (discounting the possibility of additional untagged soft leptons). Such a channel could still be populated if at least one of the following ingredients is present:

(1) Sizeable lepton number violating interactions.
(2) A hard process that is initiated by the leptonic content of the proton.

However, the first is bounded by strict low-energy constraints; see, for instance, Refs. [20,21]. For the second, the leptonic parton distribution functions (PDFs) are suppressed compared to quark or gluon initiated processes as they rely on the splitting function of the photon. The photon density in the proton is low and the splitting adds one more power of the fine-structure constant, α_{EM}. Early work on lepton PDFs can be found in Refs. [22,23]. A higher order calculation has recently been performed in Ref. [24].

Before turning to the details of the proposed search, we first discuss existing single-lepton searches in the literature. Among early experimental work, the only potentially sensitive searches are those by CMS and ATLAS for quantum black holes, such as Refs. [25,26]. However, these searches require very high multiplicity final states producing a large overall scalar sum $\sum p_T \gtrsim 2$ TeV, have no upper limit on $E_{\mathrm{T}}^{\mathrm{miss}}$, and allow for more than 1 charged lepton. In Refs. [27,28], attempts were made at model-independent searches by considering several hundreds of signal topologies including the ones we are studying here. However, since the datasets considered correspond to small integrated luminosities, and the analyses are not designed to optimally target the single-lepton final state, we expect low sensitivity to our rare signals.

Another related channel was proposed in Ref. [29] (and searched for at the LHC in Refs. [30–33]) involving a single lepton with high jet multiplicity ($1\ell + nj$, n large) but no $E_{\mathrm{T}}^{\mathrm{miss}}$ cut. This was constructed to be sensitive to several new physics scenarios which may escape high $E_{\mathrm{T}}^{\mathrm{miss}}$ searches. These include lepton number conserving models, in which case the possibly present $E_{\mathrm{T}}^{\mathrm{miss}}$ from neutrinos is diluted due the large number of final state objects. In later work, Ref. [34] demonstrated how such a channel can play a pivotal role in closing the last remaining gaps in natural supersymmetric theories. But the channel is sensitive to more generic models of new physics as well, e.g., composite Higgs models, models producing top-rich final states, or even more exotic phenomena involving high-scale nonperturbative effects.

We propose to go beyond this earlier work by focusing on the related but orthogonal final state: $1\ell + nj$, *n small*. The main difference is that we allow for a significantly lower multiplicity in the final state. The low $E_{\mathrm{T}}^{\mathrm{miss}}$ in such scenarios is not due to dilution as above, but due to lepton number violating processes and/or lepton PDFs. Thus, unlike above, we require a strict upper limit on $E_{\mathrm{T}}^{\mathrm{miss}}$. In Sec. IV, we define two separate search regions to cover what we think are the most relevant scenarios missed so far.

Very recently, Ref. [35] demonstrated that a specific example of the above—a final state with one energetic charged lepton, low $E_{\mathrm{T}}^{\mathrm{miss}}$, and exactly one energetic jet—may probe large unexplored regions of the leptoquark parameter space at the LHC.[2] The s-channel leptoquark resonance is produced via the leptonic PDFs of the proton, mimicking the production at HERA [37–39]. While the result may seem surprising at first due to the suppressed lepton PDFs, the point is that the s-channel resonance has double the kinematic reach compared to leptoquark pair production, and smaller suppression from the leptoquark coupling compared to the Drell-Yan mode. Thus, it can complement these modes [40] by probing regimes where the leptoquark mass is beyond the pair production threshold, while the leptoquark coupling is not large enough for Drell-Yan to be effective. Further, it has a far cleaner signature and a dynamic boost compared to other single production modes. This idea forms the basis for the work that follows: how can these single-lepton searches be generalized to exploit a wide range of new physics appearing in s-channel resonances.

Searches for $1\ell + nj$ with n small are yet to be performed. These would not only target leptoquarks but more generally theories that contain lepton number violation, or even some new interaction between leptons and quarks, such as a heavy partially leptophilic Z' [41]. As an example of the former we will consider R-parity violating SUSY in what follows.

III. AN APPLICATION TO R-PARITY VIOLATING SUPERSYMMETRY

RPV is the most general realization of the minimal supersymmetric Standard Model (MSSM) where, with the minimal field content, all renormalizable operators allowed under the Standard Model (SM) gauge symmetries are

[1]There can be additional soft objects from the showering but they will not affect the analysis.

[2]Also see Ref. [36] for a generalization to the case of third-generation leptons and jets.

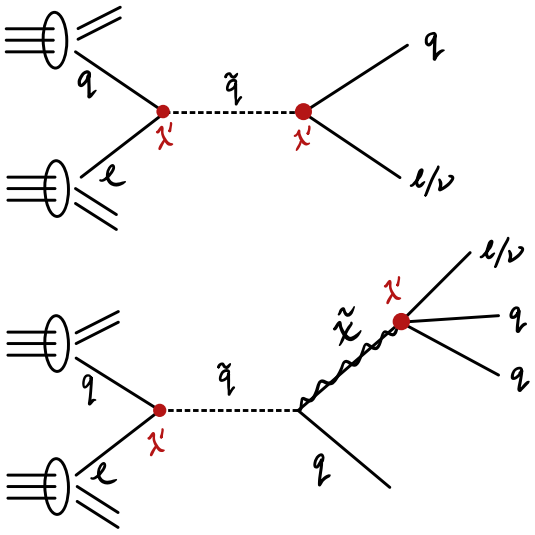

FIG. 1. Resonant squark produced via the $\lambda'_{ijk}L_iQ_j\bar{D}_k$ operator at the LHC followed by its direct decay mode (top) and decay via an example of a gauge-cascade mode (bottom). Here $\tilde{\chi}$ denotes a chargino or neutralino, lighter than the squark.

permitted [42]. This has immediate phenomenological consequences, allowing for lepton- and baryon number violating operators. However, a subset must be prohibited (for example, through a discrete symmetry) to ensure the stability of the proton [20,43–48]. In the MSSM, the imposed discrete symmetries [49,50]—e.g., R-parity—prohibit the entire set of lepton- and baryon number violating operators.

Allowing some of the RPV terms changes the phenomenology compared to the MSSM in two drastic ways: (a) the lightest supersymmetric particle (LSP) is unstable, and (b) Single production of supersymmetric particles is possible. The latter not only improves our kinematic reach but also provides a mechanism for overcoming the suppression from the lepton PDFs.

The complete superpotential for the RPV-MSSM is given by,

$$W = W_{\rm MSSM} + W_{\rm LNV} + W_{\rm BNV}, \tag{1}$$

where $W_{\rm MSSM}$ is the usual MSSM superpotential—for details see Ref. [44]—and

$$W_{\rm LNV} = \frac{1}{2}\lambda_{ijk}L_iL_j\bar{E}_k + \lambda'_{ijk}L_iQ_j\bar{D}_k + \kappa_iH_uL_i, \tag{2}$$

$$W_{\rm BNV} = \frac{1}{2}\lambda''_{ijk}\bar{U}_i\bar{D}_j\bar{D}_k, \tag{3}$$

are the new interactions that explicitly violate R-parity. In the above, $L(Q)$ and $\bar{E}(\bar{U},\bar{D})$ refer to the lepton (quark) $\mathrm{SU}(2)_L$ doublet and singlet chiral superfields from the MSSM, respectively, while H_u, H_d label the $\mathrm{SU}(2)_L$ doublet Higgs chiral superfields. The λ's, are dimensionless coupling constants; the κ's are dimension-one mass parameters. All gauge indices are suppressed but we explicitly write the generational ones: i, j, $k = 1$, 2, 3, with a summation implied over repeated labels.

Consider just a single LQD operator in the superpotential, e.g., $\lambda'_{111}L_1Q_1\bar{D}_1$. The simplest possibility leading to a single-lepton signal via this operator requires a spectrum with only a light squark, $\tilde{d}_R$ or $\tilde{u}_L$. Given no other supersymmetric particles lighter than the squark, and taking into account the lepton PDFs, the dominant process is an s-channel squark resonance, illustrated in the top diagram of Fig. 1. Here the squark decays back to the initial state, as it is the LSP. This is analogous to the scalar leptoquark scenarios considered in Ref. [35], leading to a final state comprised of a single lepton plus one jet. In contrast to leptoquark models, supersymmetry typically predicts new states lying below the squark masses [51,52], such that the squark would cascade via gauge couplings, typically all the way down to the LSP. In Table I we list possible final state signatures for $\tilde{d}_R$ as a function of the particular state lying below the squark mass. The branching ratios into these final states is determined via the relative size of the RPV coupling versus the gauge couplings, as well as details of the mass spectrum, see Refs. [53–55]. A canonical

TABLE I. Decay chains and final state signatures resulting from a resonantly produced down-type squark ($\tilde{d}_R$) in the case of $\lambda' \neq 0$. The first column indicates the supersymmetric particle involved in the final step of the decay chain, which is typically the LSP. We give a representative decay chain for each case that populates the single-lepton channel, as well as the total signature in the final column. $(*)$ indicates possibly off-shell.

Cascade end	Example decay chain	Final state signature
Bino ($\tilde{B}$)	$\tilde{d}_R \to \tilde{B} + 1j$	$1\ell + 3j$
Wino ($\tilde{W}$)	$\tilde{d}_R \to \tilde{g}^{(*)} + 1j \to \tilde{q}_L^{(*)} + 2j \to \tilde{W}^0/\tilde{W}^\pm + 3j$	$1\ell + 5j$
Gluino ($\tilde{g}$)	$\tilde{d}_R \to \tilde{g} + 1j$	$1\ell + 3j$
Doublet squark ($\tilde{q}_L$)	$\tilde{d}_R \to \tilde{g}^{(*)} + 1j \to \tilde{q}_L + 2j$	$1\ell + 3j$
Up-type singlet squark ($\tilde{u}_R$)	$\tilde{d}_R \to \tilde{g}^{(*)} + 1j \to \tilde{u}_R + 2j$	$1\ell + 5j$
Doublet charged slepton ($\tilde{e}_L$)	$\tilde{d}_R \to \tilde{g}^{(*)} + 1j \to \tilde{q}_L^{(*)} + 2j \to \tilde{W}^{0(*)} + 3j \to \tilde{e}_L + 1\ell + 3j$	$1\ell + 5j$
Sneutrino ($\tilde{\nu}_L$)	$\tilde{d}_R \to \tilde{g}^{(*)} + 1j \to \tilde{q}_L^{(*)} + 2j \to \tilde{W}^{\pm(*)} + 3j \to \tilde{\nu}_L + 1\ell + 3j$	$1\ell + 5j$
Singlet charged slepton ($\tilde{e}_R$)	$\tilde{d}_R \to \tilde{B}^{(*)} + 1j \to \tilde{e}_R + 1\ell + 1j$	$3\ell + 3j$

example is an LSP bino-like neutralino [56] giving rise to the extended decay chain depicted in the bottom diagram of Fig. 1. Upon its production from the squark, the bino-like neutralino decays via the RPV operator resulting in a final signature with three jets plus the desired single lepton.

Surveying the final states in the last column of Table I, we observe that the single-lepton channel can be populated irrespective of the supersymmetric particle involved in the final step of the decay cascade. The only exception is a decay chain featuring a light charged slepton $\tilde{e}_R$, where two additional charged leptons result.[3] There are however limitations to this analysis. As stated above the cascade details depend sensitively on the mass spectrum, as well as the size of the RPV coupling, λ', relative to the gauge couplings [54]. Fortunately, the latter does not modify the above conclusions. The large value of the strong coupling means that additional steps in the decay chains typically only increase jet multiplicity. Therefore, the single-lepton channel provides a sensitive probe irrespective of the model details, allowing us to implement a largely model-independent search strategy. We now turn to the details of how such a strategy can be implemented at the LHC.

IV. IMPLEMENTATION

We first organize the framework of our analysis in a way that allows us to be model independent. We then discuss our analysis strategy in detail, describing the signal regions and the main backgrounds involved.

A. Framework

In order to probe the RPV model, and other new physics scenarios that populate the single-lepton channel, it is useful to separate it into two distinct signatures: (a) $1\ell + 1j$ (`SR_ej`), and $1\ell + (\geq 3j)$ (`SR_e3j`). The branching ratios satisfy:

$$\mathrm{BR}(1\ell + 1j) + \mathrm{BR}(1\ell + \geq 3j) + \mathrm{BR}(\mathrm{other}) = 1. \quad (4)$$

Here, $\mathrm{BR}(X)$ refers to the branching ratio for the resonantly produced squark to decay into the final state X. $\ell = e$ or μ, and j is any (light) SM jet. Direct decays of the squark via an LQD coupling contribute to $\mathrm{BR}(1\ell + 1j)$, just like a leptoquark. From Table I, we see that the $\mathrm{BR}(1\ell + \geq 3j)$ channel gives us almost complete coverage of the possible cascade modes. BR (other) takes into account the squark decays *not* covered by the single-lepton channel, e.g., as in the last line of Table I.[4] The separation as in Eq. (4) allows us to experimentally distinguish between pure scalar leptoquark theory and a more complicated spectrum and decay pattern as for example in RPV supersymmetry.

Analytic expressions exist for the RPV-SUSY 2- or 3-body final states contributing to the branching ratios appearing in Eq. (4) [60]. For the more complicated decay chains, numerical methods are necessary, see for example the tools HERWIG [61,62], SPheno [63] and MadGraph5_aMC@NLO [64]. The analytic branching ratios even for the simpler decay chains are complicated expressions of the relevant supersymmetric parameters. Thus, we take the branching ratios in Eq. (4) as our free parameters. This also underlines our model-independent approach, as these branching ratios could easily be computed in any other model leading to the cascade decay of a resonance.

We now discuss the specifics of the search strategy, targeting the two signal regions $1\ell + 1j$ (`SR_ej`) and $1\ell + (\geq 3j)$ (`SR_e3j`).

B. Signal region: `SR_ej`

The $1\ell + 1j$ mode for a squark corresponds exactly to a decaying single leptoquark, as investigated in Ref. [35]. We briefly review this, and implement it analogously. We require one negatively charged electron or muon,[5] and one light jet and label the signature as `SR_ej`. Since we expect the mass of the squark decaying into the lepton and jet to be $\mathcal{O}(1\ \mathrm{TeV})$, we impose rather strict requirements on the transverse momentum of both objects:

$$p_{\mathrm{T}}(\ell), \qquad p_{\mathrm{T}}^{\mathrm{jet}} > 500\ \mathrm{GeV}, \quad (5)$$

with a pseudorapidity cut, $|\eta| < 2.5$. Z-boson, top quark, and QCD backgrounds are reduced by imposing a veto on events with an extra lepton with $p_{\mathrm{T}} > 7$ GeV (and $|\eta| < 2.5$), or an extra jet with $p_{\mathrm{T}} > 30$ GeV (and $|\eta| < 2.5$). W-boson backgrounds are reduced by requiring $E_{\mathrm{T}}^{\mathrm{miss}} < 50$ GeV.

With the above basic cuts, two non-negligible backgrounds remain: single W^- production in association with jets (with the W^- decaying leptonically), and QCD multijet production, where one of the jets is misidentified as a lepton. In Ref. [35] the other backgrounds are plotted; they constitute less than $\mathcal{O}(5\%)$ of the total background in the major part of the phase space. We thus neglect them here. See also the cutflow table corresponding to the benchmark point of Eq. (8) in Table II.

The strategy for this signal region is to look at the invariant mass distribution formed by the leading lepton

[3]The case of additional leptons is more constrained by existing searches, see Ref. [34].

[4]An extended RPV sector with multiple nonzero couplings could lead to further squark decays, possibly contributing to BR (other). However, note the strict bounds on products of couplings from flavor changing neutral currents [21,57] and from proton decay [58,59].

[5]The positively charged lepton mode is slightly PDF suppressed, by the different luminosities of u- and d-quarks in the proton. Of course, at high energies, one must also consider how well charge identification can perform but we consider 100% efficiency here.

TABLE II. Cutflow corresponding to the basic cuts for SR_ej for 100 fb^{-1} of integrated luminosity. For the signal, the generator level cuts are the default MadGraph5_aMC@NLO values. For the associated W^- background, an additional cut of $p_T > 400$ GeV on the lepton has been applied. This is why it appears as if the lepton p_T cut affects the signal more than the background, degrading the signal to background ratio; this is a superficial effect. Lastly, the final veto step actually dilutes the signal ratio against the W^-+ jets BG. However, as explained in the main body, it is crucial in reducing the Z-boson, top and QCD backgrounds, which would otherwise dominate over the signal.

Cuts	Signal	$W^- +$ jets
Generator Level	91	11050
Leading lepton $p_T > 500$ GeV	37	3274
Leading jet $p_T > 500$ GeV	34	2183
$E_T^{miss} < 50$ GeV	21	750
Veto	10	278

TABLE III. Cutflow corresponding to the basic cuts for SR_e3j for 100 fb^{-1} of integrated luminosity. For the signal, the generator level cuts are the default MadGraph5_aMC@NLO values. For the associated W ($t\bar{t}$) background, extra cuts are used on top of the default ones: lepton $p_T > 150$ GeV, $iH_T > 800$ GeV (500 GeV), and $E_T^{miss} < 50$ GeV. Consequently, the detector level cuts appear to suppress the signal more strongly that the background.

Cuts	Signal	$W +$ jets	$t\bar{t}$
Generator Level	130	9565	2615
b veto	118	8389	539
Leading lepton $p_T > 200$ GeV, Extra lepton veto	32	3787	114
$p_T^{jet\,1,2,3} > 50$ GeV	29	2562	72
$iH_T > 900$ GeV	25	1892	26
$S_T > 1500$ GeV	21	935	10
$E_T^{miss} < 50$ GeV	12	417	3

and jet. The signal is expected to peak in a narrow region around the squark mass, while the background falls monotonically. We present numerical results for our benchmark scenario in Sec. V.

C. Signal region: SR_e3j

In this signal region we require one charged electron or muon (or their antiparticles), and at least three jets; we label it as SR_e3j. Here, we do not restrict ourselves to only the negatively charged leptons as the cascades in Table I involve Majorana fermions, e.g., the neutralinos or the gluino, which decay into a final state or its charge conjugate with equal probability.

We implement the following basic cuts for the leading lepton and the three leading jets:

$$p_T(\ell) > 200 \text{ GeV}, \tag{6}$$

$$p_T^{jet_1}, p_T^{jet_2}, p_T^{jet_3} > 50 \text{ GeV}, \tag{7}$$

with all objects required to have $|\eta| < 2.5$. As before, to reduce Z-boson backgrounds, we veto events with an extra lepton (satisfying $p_T > 7$ GeV and $|\eta| < 2.5$). Top backgrounds are reduced by a b-jet veto. However, unlike the SR_ej case, we do not veto events with extra light jets.

A useful category of cuts is provided by scalar sums of energies of the final state objects. These mostly depend on the energy scales involved and not on the cascade details. We employ two: the sum of $|p_T|$ of all reconstructed jets, H_T; and the total scalar sum of the $|p_T|$ of all reconstructed objects and the missing transverse energy, S_T. We require $H_T > 900$ GeV, and $S_T > 1500$ GeV. We reduce the W-boson background by requiring $E_T^{miss} < 50$ GeV.

With the above cuts, to a good approximation, the main backgrounds are associated single W, associated $t\bar{t}$, and QCD multijet production. One can find the relevant backgrounds plotted as a function of H_T in Ref. [65], where the analysis has some overlap with the cuts we make. There, one can see that the other backgrounds make up less than $\mathcal{O}(5\%)$ of the total background. Actually, in our case, the $t\bar{t}$ background is also expected to be much smaller than the associated W one. In general, the former only becomes significant relative to the latter, when one requires a large number of jets in the final state, or if the jets have lower energies.[6] Since our final state of interest only has a few jets and these are energetic, we will focus on the $W+$ jets and the QCD multijet backgrounds. See also the cutflow table corresponding to the benchmark point of Eq. (8) in Table III; we show the $t\bar{t}$ numbers too for comparison, but we do not include them in our numerical studies.

We note that in designing the above cuts, we have chosen generality over optimality. The kinematical configuration of the final state objects is decided by the details of the gauge cascade, which in turn depend on the SUSY mass spectrum, to which we choose to remain blind in our approach. Finally, our strategy is to look at invariant mass distributions for the squark and the particle at the end of the cascade (typically the LSP).

D. Other signatures

So far we have only focused on resonant squark production at the LHC via the lepton PDFs. Here we briefly mention that a nonzero λ', as we have been considering, can also lead to resonant *slepton* production via quark PDFs.[7] The direct decay gives a resonance bump

[6]For instance, see the relative contributions of the two backgrounds (in the zero b-jet tag bin) as a function of the number of jets and the energies required in Refs. [30,32].

[7]Note that the bound on λ'_{111} from neutrinoless double beta decay [57,66] is strongly model dependent and is not relevant for a heavy neutralino and gluino as we discuss here.

in the 2-jet cross section. The cascade decay via a neutralino LSP leads to the promising signature of like-sign dileptons [67–69]. More relevant to the search presented here is the decay of the neutralino to a neutrino and 2 jets, giving an overall signature of 1 lepton +2jets and $E_{\mathrm{T}}^{\mathrm{miss}}$ from a neutrino. However, with 2 jets and possibly a large amount of $E_{\mathrm{T}}^{\mathrm{miss}}$, this is orthogonal to the search at hand, and we do not further consider it. We now present some numerical results.

V. RESULTS AND DISCUSSION

A. Numerical setup

For the results presented here, we have generated event samples corresponding to center-of-mass energy $\sqrt{s} = 13$ TeV, using the program MadGraph5_aMC@NLO [64] linked to PYTHIA 8.2 [70] for showering and/or decays. Once showered, the event samples are passed through our analysis which has been implemented in CheckMATE 2 [71–75]; detector effects are accounted for by the linked DELPHES 3 [76] component. For all electrons in our analysis, we have used the ATLAS "Tight" criterion implemented in CheckMATE 2 while for jets we use the anti-k_{T} algorithm implemented in FastJet, which is the CheckMATE 2 default. We choose the cone size $\Delta R = 0.4$.

We have generated the signal samples using the `UFO RPV-SUSY` model file available at Ref. [77]. We use the lepton PDFs calculated in Ref. [24], which have been implemented in the LHAPDF [78] setup. One subtle point is the handling of initial state leptons during showering; here we have followed the prescription described in Ref. [35]. Note that we have only generated the signal sample at leading order (LO). Both NLO (next-to-leading order) QCD and NLO QED corrections [79,80] relying on the photon PDF can be significant, but they contribute with opposite signs and comparable magnitudes, leading to a milder-than-expected net correction of $\mathcal{O}(10\%)$ to the LO cross section [81]. This would be important to consider in precision studies; this is not the focus of the present work.

We define the following benchmark scenario that we use to present most of our results in this section:

$$\lambda'_{111} = 0.4, \quad M_{\tilde{u}_L} = M_{\tilde{d}_R} = 2 \text{ TeV}, \quad M_{\mathrm{LSP}} = 1 \text{ TeV}. \tag{8}$$

The above choice is motivated by current LHC squark limits, while the LSP can be drastically lighter [82]. The value of λ'_{111} is chosen to lie near current constraints from low-energy experiments [57,83]. We stress that in the above we do not specify the nature of the LSP, or the details of the SUSY parameters. Instead, as mentioned earlier, we treat the branching ratios as the free variables that capture all the relevant information. We do however assume that no RPV coupling other than λ'_{111} contributes to our two signal regions.

For the W^- + jets background corresponding to `SR_ej`, we use MadGraph5_aMC@NLO to generate one electron, one anti-neutrino plus one jet at LO in QCD. We have not included the electroweak contribution. We deal with the issue of low statistics in the high-p_{T} region by implementing a generator level cut on the lepton: $p_{\mathrm{T}} > 400$ GeV, and through phase-space splicing. We split the phase space into several regions based on the p_{T} of the electron, and then glue them together at the end to get a continuous distribution. We account for NLO QCD corrections by employing a k-factor. In general, k-factors are phase-space dependent; to ensure we get a value that is appropriate for our region of interest, we use MadGraph5_aMC@NLO to calculate the total cross sections for the above process at LO and NLO in the phase-space region where the electron has $p_{\mathrm{T}} > 400$ GeV. Taking the ratio, this gives us a k-factor of 1.61. We have validated our obtained background against Ref. [35] and find good agreement. We depict the cutflow corresponding to the cuts of `SR_ej` for the background and the benchmark signal point in Table II.

For the QCD multijet background, ATLAS and CMS usually use data-driven studies over simulation. We use the numbers provided in Ref. [35]; these have been read off from a data-driven study by ATLAS in Ref. [84].

For the W+ jets background in the case of `SR_e3j`, we use MadGraph5_aMC@NLO linked to PYTHIA 8.2 to generate one electron, one anti-neutrino plus up to 3 jets (and the charge conjugated process) at LO accuracy in QCD using the MLM prescription [85–87], with the xqcut scale set to 70 GeV; we have checked that this gives smooth differential jet rate (DJR) distributions for our process and energy scale [88]. We have not included the electroweak contribution. To obtain sufficient statistics in the tail of the distribution, we again use generator level cuts: lepton $p_{\mathrm{T}} > 150$ GeV, $iH_{\mathrm{T}} > 800$ GeV, and $E_{\mathrm{T}}^{\mathrm{miss}} < 50$ GeV, and phase-space splicing and gluing—this time relying on splits based on the iH_{T} (inclusive scalar sum of jet energies) variable available in MadGraph5_aMC@NLO.

We account again for NLO effects by employing a k-factor. Here we take the ratio of the total cross sections for associated W production at NLO and LO with the default MadGraph5_aMC@NLO cuts which gives us a k-factor of 1.286. We expect this to be an overestimate since the k-factor decreases both in the relevant region of phase space [89,90], as well as when requiring a larger number of associated jets. This avoids the computationally intensive task of calculating the full NLO cross section with 3 extra partons; similar approaches have been employed by ATLAS and CMS in Refs. [91,92], and we emphasize that this produces conservative results. We depict the cutflow corresponding to the cuts of `SR_e3j` for the background and the benchmark signal point in Table III.

We do not calculate the QCD multijet background but rather include it as an extra 30% contribution to the final number of background events after our cuts. This is a very rough estimate using the background distributions plotted

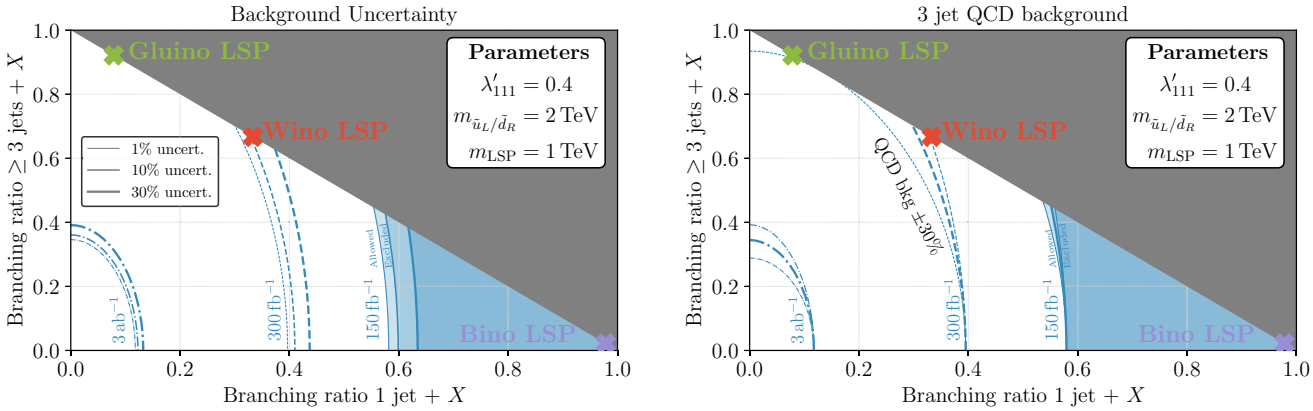

FIG. 2. Projected constraints based on integrated luminosities of $(150, 300, 3000)$ fb^{-1} shown as blue-(solid, dashed, dot-dashed) contours. These constraints are shown as a function of the branching ratios into the two channels: (i) 1 jet $+ X$, and (ii) ≥ 3 jets $+ X$ where X denotes either an electron or a neutrino. As reference points, we show the expected branching ratios for an RPV model featuring a 1 TeV gluino, bino or wino-LSP, see Sec. IV A for more details. Left: we vary the systematic uncertainty on the background predictions in both channels (1%, 10%, and 30%) showing how the exclusion limits change. Right: we study how varying the QCD background rate for the three jet channel from the assumed 30% affects our results.

in Ref. [65], and accounting for the fact that the extra missing energy cut we make in our analysis targets the W-boson more effectively than it will target multijets. We will study the importance of this assumption in Fig. 2.

For `SR_ej`, after passing the samples through the basic cuts, we look at the invariant mass distribution of the leading lepton and leading jet to reconstruct the squark mass. The width of the bins, for a narrow resonance, is determined by the experimental resolution. Here, we choose it to be approximately 10% of the invariant mass.

For `SR_e3j`, we first reconstruct the invariant mass distribution for the particle at the end of the cascade, choosing a rather broad binning size of 400 GeV.[8] For events in each bin, we then reconstruct the squark mass by looking at the invariant mass distribution formed by all reconstructed objects, selecting the binning width to be approximately 10% of the invariant mass.

Finally, we calculate the potential exclusion significance [94] for both `SR_ej` and `SR_e3j` by reading off the signal and background numbers in each squark bin and select the highest value as the resulting significance.

B. Search sensitivity

We present the projected 95% confidence level (CL) exclusion limits corresponding to the benchmark scenario, Eq. (8), for the current data on tape (150 fb^{-1}), as well as projections for the HL-LHC using 300 fb^{-1} and 3 ab^{-1} of integrated luminosity in Fig. 2.[9] The projections are shown in a model-independent manner as a function of the branching ratios of Eq. (4). We depict on the figure where a supersymmetric model with a 1 TeV gluino-, wino-, or bino-like LSP, respectively, would lie, assuming the resonantly produced squark is the NLSP. Here we have assumed that λ'_{111} is the only nonzero RPV coupling, and no other decays are open. Therefore, they all lie on the line,

$$\text{BR}(X + 1j) + \text{BR}(X + \geq 3j) = 1. \tag{9}$$

We have combined the decay modes corresponding to a charged lepton and a neutrino into a single branching ratio, namely $X \equiv \ell$ or ν. This is convenient for the normalization since in the RPV-MSSM, neglecting lepton masses, the two modes are symmetric to a very good approximation. Our analysis still targets only the charged lepton, e.g., $\text{BR}(1\ell + 1j) = 0.5 \times \text{BR}(X + 1j)$.

We emphasize that Fig. 2 can be used to reinterpret the results for any model. For example, for an additional significant nonzero λ_{121}, we would obtain decays with more than 1 charged lepton in the final state, resulting in a nonzero BR(other),

$$\text{BR}(X + 1j) + \text{BR}(X + \geq 3j) < 1. \tag{10}$$

Such a model would lie in the lower left triangle.

Figure 2 shows that, even with current data, the single-lepton channel can probe large regions of the RPV model space (for instance, the Bino LSP scenario) corresponding

[8] In a spectrum-blind approach, one does not know which final state objects originate from the decay of the cascade-end particle. Experimentally this requires looking at multiple distributions formed by combinations of the reconstructed electron and jets; see, for instance, Ref. [93]. Here we work with simulations where the cascade-end is fixed which means we do not go through this procedure. However, our chosen broad binning size compensates to account for possible inefficient matching between the reconstructed objects and the true parton level decay products.

[9] This is assuming no discovery is imminent at the projected reach.

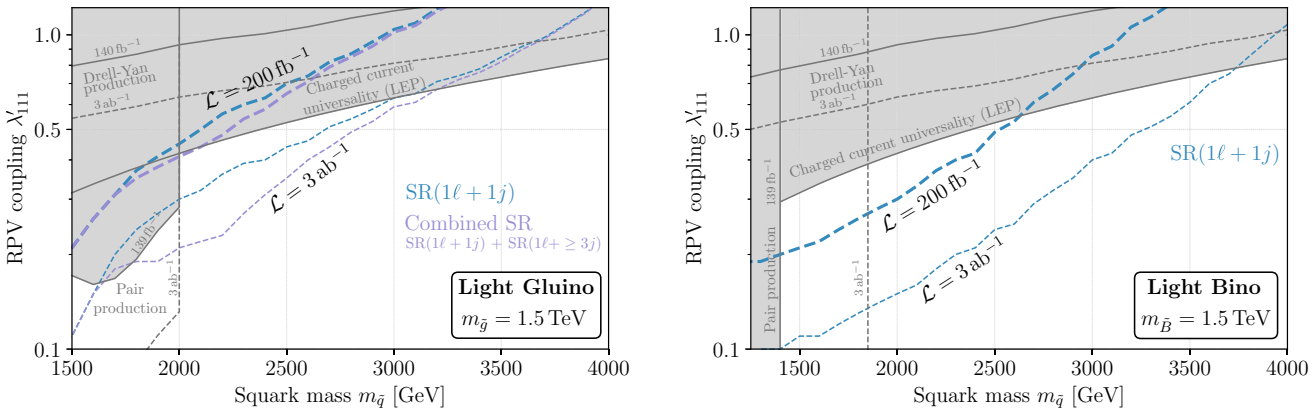

FIG. 3. The search sensitivities of the single-lepton channel for the light gluino (left) and light bino (right) scenarios corresponding to two different integrated luminosities: 200 fb^{-1} (thick lines) and 3 ab^{-1} (thin lines). For the gluino case, the reach of the SR_ej search is shown in turquoise and the combined reach of SR_ej + SR_e3j is shown in purple. For the bino case we just show the reach of SR_ej. In both plots we show in gray the area excluded by existing experiments: Drell-Yan [95], charged current universality [96] and squark pair production [97–99], with each region labeled by its corresponding cause of exclusion. Finally, we show the projected limits assuming $\mathcal{L} = 3$ ab^{-1} for both Drell-Yan, and squark pair production as dashed gray lines.

to the benchmark point, allowing us to go beyond existing bounds. By the end of HL-LHC runs, nearly the whole space of models corresponding to the benchmark can be probed.

The figure also studies how systematic uncertainties, and our assumption about the QCD background in SR_e3j affect our results.

In a next step, we study how the exclusion limits depend on the mass of the squarks and the RPV coupling. We assume $\tilde{u}_L$ and $\tilde{d}_R$ are mass-degenerate, and consider two simplified setups, corresponding to a 1500 GeV gluino, and a 1500 GeV bino, respectively, with the rest of the SUSY spectrum decoupled. As before, we also require λ'_{111} to be the only nonzero RPV coupling. The results for the light gluino (left) and light bino (right) scenarios are shown in Fig. 3, neglecting systematic uncertainties. We summarize the results of Fig. 3 in Table IV, depicting the most stringent current bound on λ'_{111} and comparing it with the bound implied by the single-lepton search.

The turquoise line corresponds to the signal region SR_ej while the purple line shows the combination of both signal regions SR_ej + SR_e3j. The thick lines show the search sensitivity for an integrated luminosity of $\mathcal{L} = 200$ fb^{-1} while the thinner lines correspond to $\mathcal{L} = 3$ ab^{-1}. The figure also depicts other current relevant bounds as shaded gray regions. Currently the most stringent constraints at large squark masses come from charged current universality measurements at LEP [96]. We have also recast limits from existing pair production [97] and Drell-Yan searches [95], as well as a projection of their reach at HL-LHC determined by assuming $\mathcal{L} = 3$ ab^{-1}.

For the light gluino case, the most constraining current exclusion limits are from charged current universality, reaching values of $\lambda'_{111} > 0.3$ for $m_{\tilde{q}} \sim 1500$ GeV and $\lambda'_{111} > 0.8$ for $m_{\tilde{q}} \sim 4000$ GeV, and from squark pair production that is powerful for low masses, reaching $\lambda'_{111} > 0.16$ for masses of the squarks between 1600–1700 GeV. The pair-production exclusion region below about 2000 GeV has a slope because the search relies on the direct decay mode of the squark; higher mass squarks need a higher RPV coupling to have a sufficient branching ratio for this mode. For squark masses between 1500–1600 GeV, the exclusion deteriorates slightly. The experimentally observed data in this regime are above the expected ones while for higher masses, both observed and expected match; see Ref. [97]. The search only excludes squark masses up to 2000 GeV. Thus, the shaded area extends vertically at this point.

We see that the single-lepton channel probes phase-space regions complementary to those probed by pair production and Drell-Yan, as explained in Sec. II. Further, it has the potential to compete with/outdo the existing charged

TABLE IV. Summary of Fig. 3. The table compares the best existing bounds (from pair production, Drell-Yan, and LEP) on λ'_{111} and compares it to the bounds implied by the single-lepton search from Fig. 3 for various squark masses, for the light gluino (bino) scenarios. For values marked with an asterisk, the perturbativity constraint is stronger.

$M_{\tilde{u}_L} = M_{\tilde{d}_R}$ (TeV)	λ'_{111} Current bound	λ'_{111} Single lepton channel	
		200 fb^{-1}	3 ab^{-1}
1.5	0.17 (0.315)	0.21 (0.21)	0.11 (0.11)
2	0.28 (0.42)	0.41 (0.3)	0.21 (0.15)
2.5	0.525	0.65 (0.48)	0.35 (0.24)
3	0.63	1.0 (0.83)	0.58 (0.39)
3.5	0.735	1.49* (1.37*)	0.8 (0.59)

current universality constraints, with the added advantage of being a direct search.

For a light gluino, the squarks can have a significant branching ratio into the cascade mode since it proceeds via the strong coupling. To see this, we depict the sensitivity contour corresponding to SR_ej alone (turquoise), and to SR_ej + SR_e3j combined (purple). For low squark masses, SR_e3j is relatively unimportant since the squarks have no phase space to decay into the gluino; the direct decay dominates. As the mass increases, the relative importance of SR_e3j grows. At very high masses, it becomes less important again because the large λ'_{111} coupling—required to have a sufficiently high signal rate—leads to the direct decay rate increasing as well.

The light bino case is shown in the right plot of Fig. 3. Current searches such as Drell-Yan and charged current universality behave as in the gluino LSP case and so they cover almost the same parameter space. However, the squark pair production only reaches values up to 1400 GeV. As the gluino is now decoupled, the contribution due to t-channel gluino exchange is missing leading to a smaller cross section. Further, there is no dependence on the coupling since, with the bino kinematically inaccessible in this region, the squark dominantly decays directly with branching ratio nearly 1.

As before, the single-lepton channel is complementary to the existing searches, extending the potential reach. However, the only mode with power of exclusion here is SR_ej. The branching ratio of the cascade mode via the bino is small leading to a low sensitivity of SR_e3j. Correspondingly, we have not included the SR_e3j curves. In comparing with the gluino LSP case on the left, we see that the single-lepton channel excludes more parameter space here. This is because of the higher branching ratio of the direct decay, contributing to SR_ej; this mode has a cleaner signature and hence higher exclusion potential than SR_e3j.

We note that our proposed search outperforms high-luminosity projections of the searches based on Drell-Yan and squark pair production (see dashed gray lines in Fig. 3). The Drell-Yan constraints begin to be competitive at very high masses; although they are still surpassed by constraints from LEP measurements. On the other hand, for pair production, the reach improves for low squark masses, reaching $m_{\tilde{q}} = 2$ TeV in the light gluino case, and $m_{\tilde{q}} = 1.8$ TeV in the light bino case. These projections are based on current searches, which place a strict cut of 2 TeV on the squark masses. This limits the sensitivity of our projections. Nevertheless, this last search is powerful for low masses exhibiting strong complementarity with the search proposed in this work.

An interesting observation is that SR_ej is quite powerful even in cases where the squark has low BR into the direct mode, e.g., the light gluino scenario, left plot in Fig. 3. This shows that a simple resonance $1\ell + 1j$ search is also a powerful probe of the entire RPV space, even with a more complicated spectrum; not just the leptoquark-like scenario. On the other hand, SR_e3j apart from extending the reach of the searches (particularly at high-luminosities), will be crucial to distinguish between leptoquarks and squarks in case of a discovery.

It is also important to emphasize that even though we have considered simplified setups, with most of the SUSY spectrum decoupled, our results are more general. For instance, we would realistically expect the sleptons and electroweakinos to also be light in the light gluino case. In such a scenario, new gauge-cascade chains can open up for the resonant squark, thus diluting the direct and gluino decay modes. However, the signals from these distinct chains will simply add up with those from the gluino mode in the SR_e3j bin, as long as the end point of all the cascades is the same. This is exactly what happens, for instance, for small RPV couplings, where all gauge-cascade chains end in the LSP.

Finally, we note that one can perform completely analogous studies for LQD operators involving second generation fermions. For a coupling with a second generation lepton, e.g., λ'_{211} we expect the limits to weaken only slightly as the muon PDFs are only mildly suppressed relative to the electron ones [24]. The case of second generation quarks is slightly more involved. For λ'_{111} the dominant production mode is $eu \to \tilde{d}$ versus $ed \to \tilde{u}$, roughly in the ratio 2:1. Thus, we would expect the case λ'_{112} to be only mildly suppressed compared to our present analysis, whereas the case λ'_{121} to be more suppressed. But both should still be feasible; see Ref. [35] for quantitative estimates.

VI. CONCLUSIONS

In this paper we have shown that the single-lepton channel is a promising signature in the search for new physics beyond the Standard Model. We have considered two specific versions of this channel: (a) a single first or second generation charged lepton, exactly 1 jet and low missing transverse energy, which we denoted SR_ej, and (b) a single first or second generation charged lepton, at least 3 jets, and low missing transverse energy, SR_e3j. Utilizing the lepton parton distribution functions (PDF) of the proton, we showed that the channel SR_ej is promising not only in the search for a single leptoquark or a directly decaying squark, but remains sensitive even when more complicated supersymmetric cascade decays are accessible. Further, the channel SR_e3j plays an important role in increasing both the reach and coverage in such scenarios. More importantly, it also acts as a discriminant between a bare scalar leptoquark theory versus one with a more extensive supersymmetric sector featuring kinematically accessible particles beyond just a light squark.

Although ATLAS and CMS have performed single-lepton searches associated with large jet multiplicity, see

Refs. [30–33], our proposed search covers a variety of scenarios which would not produce a sufficiently large number of jets. Beyond the question of coverage, the resonant s-channel production mechanism invoked in our analysis benefits tremendously from the forthcoming increase of luminosity at the LHC. We therefore strongly advocate that this type of search be pursued at forthcoming LHC runs, as well as emphasize the necessity of more exhaustive theoretical work surveying the opportunities that will arise in the era of High-Luminosity LHC.

ACKNOWLEDGMENTS

We thank Giulia Zanderighi for very helpful comments on their paper [35] and on the numerical implementation of the lepton PDFs, Rhorry Gauld for helpful comments about the leptonic PDFs of the proton, both Philip Bechtle and Admir Greljo for useful discussions about search strategies and other relevant limits, and lastly Simon Knapen for comments on the manuscript. The work of H. K. D. and S. N. has been supported by BMBF project Grant No. 05H18PDCA1. V. M. L. is funded by the Deutsche Forschungsgemeinschaft (DFG, German Research Foundation) under Germany's Excellence Strategy—EXC 2121 "Quantum Universe"—39083330, V. M. L. also acknowledges the financial support by Ministerio de Universidades and "European Union-NextGenerationEU/PRTR" under the Grant No. María Zambrano ZA2021-081, and the Spanish Grants No. PID2020–113775GB-I00 (AEI) and No. CIPROM/2021/054 (Generalitat Valenciana).

[1] lhc-lumi, Beam performance tracking in the CERN accelerator complex, https://bpt.web.cern.ch/lhc/ (2023).
[2] High-Luminosity Large Hadron Collider (HL-LHC): Technical design report V. 0.1, Report number CERN-2017-007-M, 2017, 10.23731/CYRM-2017-004.
[3] CMS Collaboration, First level track jet trigger for displaced jets at high luminosity LHC, Technical Report, CERN, Geneva, 2018.
[4] B. Bhattacherjee, S. Mukherjee, R. Sengupta, and P. Solanki, Triggering long-lived particles in HL-LHC and the challenges in the first stage of the trigger system, J. High Energy Phys. 08 (2020) 141.
[5] Y. Gershtein, CMS hardware track trigger: New opportunities for long-lived particle searches at the HL-LHC, Phys. Rev. D **96**, 035027 (2017).
[6] Y. Gershtein and S. Knapen, Trigger strategy for displaced muon pairs following the CMS phase II upgrades, Phys. Rev. D **101**, 032003 (2020).
[7] J. A. Evans, A. Gandrakota, S. Knapen, and H. Routray, Searching for exotic B-meson decays enabled by the CMS L1 track trigger, Phys. Rev. D **103**, 015026 (2021).
[8] Y. Gershtein, S. Knapen, and D. Redigolo, Probing naturally light singlets with a displaced vertex trigger, Phys. Lett. B **823**, 136758 (2021).
[9] R. Aaij *et al.* (LHCb Collaboration), Test of lepton flavor universality by the measurement of the $B^0 \to D^{*-}\tau^+\nu_\tau$ branching fraction using three-prong τ decays, Phys. Rev. D **97**, 072013 (2018).
[10] R. Aaij *et al.* (LHCb Collaboration), Test of lepton universality in beauty-quark decays, Nat. Phys. **18**, 277 (2022).
[11] G. W. Bennett *et al.* (Muon $g-2$ Collaboration), Measurement of the Positive Muon Anomalous Magnetic Moment to 0.7 ppm, Phys. Rev. Lett. **89**, 101804 (2002); **89**, 129903(E) (2002).
[12] G. W. Bennett *et al.* (Muon $g-2$ Collaboration), Measurement of the Negative Muon Anomalous Magnetic Moment to 0.7 ppm, Phys. Rev. Lett. **92**, 161802 (2004).
[13] G. W. Bennett *et al.* (Muon $g-2$ Collaboration), Final report of the E821 muon anomalous magnetic moment measurement at BNL, Phys. Rev. D **73**, 072003 (2006).
[14] B. Abi *et al.* (Muon $g-2$ Collaboration), Measurement of the Positive Muon Anomalous Magnetic Moment to 0.46 ppm, Phys. Rev. Lett. **126**, 141801 (2021).
[15] M. Bauer and M. Neubert, Minimal Leptoquark Explanation for the $R_{D^{(*)}}$, R_K, and $(g-2)_\mu$ Anomalies, Phys. Rev. Lett. **116**, 141802 (2016).
[16] P. Fileviez Perez, C. Murgui, and A. D. Plascencia, Leptoquarks and matter unification: Flavor anomalies and the muon $g-2$, Phys. Rev. D **104**, 035041 (2021).
[17] S. Trifinopoulos, B-physics anomalies: The bridge between R-parity violating supersymmetry and flavored dark matter, Phys. Rev. D **100**, 115022 (2019).
[18] Q.-Y. Hu, Y.-D. Yang, and M.-D. Zheng, Revisiting the B-physics anomalies in R-parity violating MSSM, Eur. Phys. J. C **80**, 365 (2020).
[19] M. Chakraborti, S. Iwamoto, J. S. Kim, R. Masełek, and K. Sakurai, Supersymmetric explanation of the muon $g-2$ anomaly with and without stable neutralino, J. High Energy Phys. 08 (2022) 124.
[20] H. K. Dreiner, An introduction to explicit R-parity violation, Adv. Ser. Dir. High Energy Phys. **21**, 565 (2010).
[21] R. Barbier *et al.*, R-parity violating supersymmetry, Phys. Rep. **420**, 1 (2005).
[22] J. Ohnemus, S. Rudaz, T. F. Walsh, and P. M. Zerwas, Single leptoquark production at hadron colliders, Phys. Lett. B **334**, 203 (1994).
[23] V. Bertone, S. Carrazza, D. Pagani, and M. Zaro, On the impact of lepton PDFs, J. High Energy Phys. 11 (2015) 194.
[24] L. Buonocore, P. Nason, F. Tramontano, and G. Zanderighi, Leptons in the proton, J. High Energy Phys. 08 (2020) 019.
[25] S. Chatrchyan *et al.* (CMS Collaboration), Search for microscopic black holes in pp collisions at $\sqrt{s} = 8$ TeV, J. High Energy Phys. 07 (2013) 178.

[26] G. Aad *et al.* (ATLAS Collaboration), Search for microscopic black holes and string balls in final states with leptons and jets with the ATLAS detector at $\sqrt{s} = 8$ TeV, J. High Energy Phys. 08 (2014) 103.
[27] ATLAS Collaboration, A model independent general search for new phenomena with the ATLAS detector at $\sqrt{s} = 13$ TeV, Report No. ATLAS-CONF-2017-001.
[28] CMS Collaboration, *MUSiC*, A model unspecific search for new physics, in pp collisions at $\sqrt{s} = 8$ TeV, Report No. CMS-PAS-EXO-14-016, 2017.
[29] M. Lisanti, P. Schuster, M. Strassler, and N. Toro, Study of LHC searches for a lepton and many jets, J. High Energy Phys. 11 (2012) 081.
[30] M. Aaboud *et al.* (ATLAS Collaboration), Search for new phenomena in a lepton plus high jet multiplicity final state with the ATLAS experiment using $\sqrt{s} = 13$ TeV proton-proton collision data, J. High Energy Phys. 09 (2017) 088.
[31] A. M. Sirunyan *et al.* (CMS Collaboration), Search for R-parity violating supersymmetry in pp collisions at $\sqrt{s} =$ 13 TeV using b jets in a final state with a single lepton, many jets, and high sum of large-radius jet masses, Phys. Lett. B **783**, 114 (2018).
[32] G. Aad *et al.* (ATLAS Collaboration), Search for R-parity violating supersymmetry in a final state containing leptons and many jets with the ATLAS experiment using $\sqrt{s} =$ 13 TeV proton-proton collision data, arXiv:2106.09609.
[33] A. M. Sirunyan *et al.* (CMS Collaboration), Search for top squarks in final states with two top quarks and several light-flavor jets in proton-proton collisions at $\sqrt{s} = 13$ TeV, Phys. Rev. D **104**, 032006 (2021).
[34] J. A. Evans, Y. Kats, D. Shih, and M. J. Strassler, Toward full LHC coverage of natural supersymmetry, J. High Energy Phys. 07 (2014) 101.
[35] L. Buonocore, U. Haisch, P. Nason, F. Tramontano, and G. Zanderighi, Lepton-Quark Collisions at the Large Hadron Collider, Phys. Rev. Lett. **125**, 231804 (2020).
[36] U. Haisch and G. Polesello, Resonant third-generation leptoquark signatures at the Large Hadron Collider, J. High Energy Phys. 05 (2021) 057.
[37] W. Buchmuller, R. Ruckl, and D. Wyler, Leptoquarks in lepton—quark collisions, Phys. Lett. B **191**, 442 (1987); **448**, 320(E) (1999).
[38] J. Butterworth and H. K. Dreiner, R-parity violation at HERA, Nucl. Phys. **B397**, 3 (1993).
[39] H. K. Dreiner and P. Morawitz, Signals for supersymmetry at HERA, Nucl. Phys. **B428**, 31 (1994); **B574**, 874(E) (2000).
[40] A. Crivellin, D. Müller, and L. Schnell, Combined constraints on first generation leptoquarks, Phys. Rev. D **103**, 115023 (2021).
[41] A. J. Buras, A. Crivellin, F. Kirk, C. A. Manzari, and M. Montull, Global analysis of leptophilic Z' bosons, J. High Energy Phys. 06 (2021) 068.
[42] S. Weinberg, Supersymmetry at ordinary energies. 1. Masses and conservation laws, Phys. Rev. D **26**, 287 (1982).
[43] L. E. Ibanez and G. G. Ross, Discrete gauge symmetries and the origin of baryon and lepton number conservation in supersymmetric versions of the standard model, Nucl. Phys. **B368**, 3 (1992).
[44] B. C. Allanach, A. Dedes, and H. K. Dreiner, R parity violating minimal supergravity model, Phys. Rev. D **69**, 115002 (2004); **72**, 079902(E) (2005).
[45] H. K. Dreiner, H. Murayama, and M. Thormeier, Anomalous flavor U(1)(X) for everything, Nucl. Phys. **B729**, 278 (2005).
[46] H. K. Dreiner, C. Luhn, H. Murayama, and M. Thormeier, Baryon triality and neutrino masses from an anomalous flavor U(1), Nucl. Phys. **B774**, 127 (2007).
[47] H. K. Dreiner, M. Hanussek, and C. Luhn, What is the discrete gauge symmetry of the R-parity violating MSSM?, Phys. Rev. D **86**, 055012 (2012).
[48] C. Csaki, E. Kuflik, and T. Volansky, Dynamical R-Parity Violation, Phys. Rev. Lett. **112**, 131801 (2014).
[49] G. R. Farrar and P. Fayet, Phenomenology of the production, decay, and detection of new hadronic states associated with supersymmetry, Phys. Lett. **76B**, 575 (1978).
[50] H. K. Dreiner, C. Luhn, and M. Thormeier, What is the discrete gauge symmetry of the MSSM?, Phys. Rev. D **73**, 075007 (2006).
[51] B. C. Allanach, A. Dedes, and H. K. Dreiner, Two loop supersymmetric renormalization group equations including R-parity violation and aspects of unification, Phys. Rev. D **60**, 056002 (1999); **86**, 039906(E) (2012).
[52] B. C. Allanach, SOFTSUSY: A program for calculating supersymmetric spectra, Comput. Phys. Commun. **143**, 305 (2002).
[53] H. K. Dreiner and G. G. Ross, R-parity violation at hadron colliders, Nucl. Phys. **B365**, 597 (1991).
[54] H. K. Dreiner, F. Staub, A. Vicente, and W. Porod, General MSSM signatures at the LHC with and without R-parity, Phys. Rev. D **86**, 035021 (2012).
[55] D. Dercks, H. Dreiner, M. E. Krauss, T. Opferkuch, and A. Reinert, R-parity violation at the LHC, Eur. Phys. J. C **77**, 856 (2017).
[56] H. K. Dreiner, S. Heinemeyer, O. Kittel, U. Langenfeld, A. M. Weber, and G. Weiglein, Mass bounds on a very light neutralino, Eur. Phys. J. C **62**, 547 (2009).
[57] B. C. Allanach, A. Dedes, and H. K. Dreiner, Bounds on R-parity violating couplings at the weak scale and at the GUT scale, Phys. Rev. D **60**, 075014 (1999).
[58] N. Chamoun, F. Domingo, and H. K. Dreiner, Nucleon decay in the R-parity violating MSSM, Phys. Rev. D **104**, 015020 (2021).
[59] A. Y. Smirnov and F. Vissani, Upper bound on all products of R-parity violating couplings λ' and $\lambda^{''}$ from proton decay, Phys. Lett. B **380**, 317 (1996).
[60] P. Richardson, Simulations of R-parity violating SUSY models, Ph.D. thesis, Oxford University, 2000, 8, arXiv:hep-ph/0101105.
[61] H. K. Dreiner, P. Richardson, and M. H. Seymour, Parton shower simulations of R-parity violating supersymmetric models, J. High Energy Phys. 04 (2000) 008.
[62] G. Corcella, I. G. Knowles, G. Marchesini, S. Moretti, K. Odagiri, P. Richardson, M. H. Seymour, and B. R. Webber, HERWIG 6: An event generator for hadron emission reactions with interfering gluons (including supersymmetric processes), J. High Energy Phys. 01 (2001) 010.
[63] W. Porod, SPheno, a program for calculating supersymmetric spectra, SUSY particle decays and SUSY particle

production at e^+e^- colliders, Comput. Phys. Commun. **153**, 275 (2003).
[64] J. Alwall, R. Frederix, S. Frixione, V. Hirschi, F. Maltoni, O. Mattelaer, H. S. Shao, T. Stelzer, P. Torrielli, and M. Zaro, The automated computation of tree-level and next-to-leading order differential cross sections, and their matching to parton shower simulations, J. High Energy Phys. 07 (2014) 079.
[65] V. Khachatryan *et al.* (CMS Collaboration), Search for supersymmetry in events with one lepton and multiple jets in proton-proton collisions at $\sqrt{s} = 13$ TeV, Phys. Rev. D **95**, 012011 (2017).
[66] M. Hirsch, H. V. Klapdor-Kleingrothaus, and S. G. Kovalenko, Supersymmetry and neutrinoless double beta decay, Phys. Rev. D **53**, 1329 (1996).
[67] H. K. Dreiner, P. Richardson, and M. H. Seymour, Resonant slepton production in hadron-hadron collisions, Phys. Rev. D **63**, 055008 (2001).
[68] H. K. Dreiner, S. Grab, M. Kramer, and M. K. Trenkel, Supersymmetric NLO QCD corrections to resonant slepton production and signals at the Fermilab Tevatron and the CERN LHC, Phys. Rev. D **75**, 035003 (2007).
[69] H. K. Dreiner and T. Stefaniak, Bounds on R-parity violation from resonant slepton production at the LHC, Phys. Rev. D **86**, 055010 (2012).
[70] T. Sjöstrand, S. Ask, J. R. Christiansen, R. Corke, N. Desai, P. Ilten, S. Mrenna, S. Prestel, C. O. Rasmussen, and P. Z. Skands, An introduction to PYTHIA 8.2, Comput. Phys. Commun. **191**, 159 (2015).
[71] D. Dercks, N. Desai, J. S. Kim, K. Rolbiecki, J. Tattersall, and T. Weber, CheckMATE 2: From the model to the limit, Comput. Phys. Commun. **221**, 383 (2017).
[72] M. Cacciari, G. P. Salam, and G. Soyez, FastJet user manual, Eur. Phys. J. C **72**, 1896 (2012).
[73] M. Cacciari and G. P. Salam, Dispelling the N^3 myth for the k_t jet-finder, Phys. Lett. B **641**, 57 (2006).
[74] M. Cacciari, G. P. Salam, and G. Soyez, The anti-k_t jet clustering algorithm, J. High Energy Phys. 04 (2008) 063.
[75] A. L. Read, Presentation of search results: The CL_s technique, J. Phys. G **28**, 2693 (2002).
[76] J. de Favereau, C. Delaere, P. Demin, A. Giammanco, V. Lemaître, A. Mertens, and M. Selvaggi (DELPHES 3 Collaboration), DELPHES 3: A modular framework for fast simulation of a generic collider experiment, J. High Energy Phys. 02 (2014) 057.
[77] https://feynrules.irmp.ucl.ac.be/wiki/RPVMSSM (accessed 2021-12-01).
[78] A. Buckley, J. Ferrando, S. Lloyd, K. Nordström, B. Page, M. Rüfenacht, M. Schönherr, and G. Watt, LHAPDF6: Parton density access in the LHC precision era, Eur. Phys. J. C **75**, 132 (2015).
[79] R. Gauld, Precise predictions for multi-TeV and PeV energy neutrino scattering rates, Phys. Rev. D **100**, 091301 (2019).
[80] A. Garcia, R. Gauld, A. Heijboer, and J. Rojo, Complete predictions for high-energy neutrino propagation in matter, J. Cosmol. Astropart. Phys. 09 (2020) 025.
[81] A. Greljo and N. Selimovic, Lepton-quark fusion at hadron colliders, precisely, J. High Energy Phys. 03 (2021) 279.
[82] V. A. Mitsou (ATLAS, CMS Collaborations), SUSY searches in ATLAS and CMS, CERN Report No. ATL-PHYS-PROC-2020-031, 2020.
[83] M. Hirsch, H. V. Klapdor-Kleingrothaus, and S. G. Kovalenko, New Constraints on R-Parity Broken Supersymmetry from Neutrinoless Double Beta Decay, Phys. Rev. Lett. **75**, 17 (1995).
[84] G. Aad *et al.* (ATLAS Collaboration), Search for Quantum Black Hole Production in High-Invariant-Mass Lepton + Jet Final States Using pp Collisions at $\sqrt{s} =$ 8 TeV and the ATLAS Detector, Phys. Rev. Lett. **112**, 091804 (2014).
[85] M. L. Mangano, M. Moretti, and R. Pittau, Multijet matrix elements and shower evolution in hadronic collisions: $Wb\bar{b} + n$ jets as a case study, Nucl. Phys. **B632**, 343 (2002).
[86] J. Alwall *et al.*, Comparative study of various algorithms for the merging of parton showers and matrix elements in hadronic collisions, Eur. Phys. J. C **53**, 473 (2008).
[87] J. Alwall, S. de Visscher, and F. Maltoni, QCD radiation in the production of heavy colored particles at the LHC, J. High Energy Phys. 02 (2009) 017.
[88] https://www.physics.sjtu.edu.cn/madgraphschool/sites/www.physics.sjtu.edu.cn.madgraphschool/files/tuto_matching.pdf (accessed 2021-12-01).
[89] J. Huston, LO, NLO, LO* and jet algorithms, Proc. Sci. RADCOR2009 (**2010**) 079 [arXiv:1001.2581].
[90] C. F. Berger, Z. Bern, L. J. Dixon, F. Febres Cordero, D. Forde, T. Gleisberg, H. Ita, D. A. Kosower, and D. Maitre, Next-to-leading order QCD predictions for W + 3-jet distributions at hadron colliders, Phys. Rev. D **80**, 074036 (2009).
[91] ATLAS Collaboration, ATLAS simulation of boson plus jets processes in Run 2, Report No. ATL-PHYS-PUB-2017-006, 2017.
[92] A. M. Sirunyan *et al.* (CMS Collaboration), Measurement of the differential cross sections for the associated production of a W boson and jets in proton-proton collisions at $\sqrt{s} = 13$ TeV, Phys. Rev. D **96**, 072005 (2017).
[93] A. M. Sirunyan *et al.* (CMS Collaboration), Search for a heavy resonance decaying to a top quark and a vector-like top quark in the lepton + jets final state in pp collisions at $\sqrt{s} = 13$ TeV, Eur. Phys. J. C **79**, 208 (2019).
[94] G. Cowan, K. Cranmer, E. Gross, and O. Vitells, Asymptotic formulae for likelihood-based tests of new physics, Eur. Phys. J. C **71**, 1554 (2011); **73**, 2501(E) (2013).
[95] A. M. Sirunyan *et al.* (CMS Collaboration), Search for resonant and nonresonant new phenomena in high-mass dilepton final states at $\sqrt{s} = 13$ TeV, J. High Energy Phys. 07 (2021) 208.
[96] V. D. Barger, G. F. Giudice, and T. Han, Some new aspects of supersymmetry R-parity violating interactions, Phys. Rev. D **40**, 2987 (1989).
[97] G. Aad *et al.* (ATLAS Collaboration), Search for pairs of scalar leptoquarks decaying into quarks and electrons or muons in $\sqrt{s} = 13$ TeV pp collisions with the ATLAS detector, J. High Energy Phys. 10 (2020) 112.
[98] W. Beenakker, S. Brensing, M. n. Kramer, A. Kulesza, E. Laenen, L. Motyka, and I. Niessen, Squark and gluino hadroproduction, Int. J. Mod. Phys. A **26**, 2637 (2011).
[99] S. Bornhauser, M. Drees, H. K. Dreiner, and J. S. Kim, Electroweak contributions to squark pair production at the LHC, Phys. Rev. D **76**, 095020 (2007).